Enquiring Electronic Structure Using Quantum Computers: Hands on Qiskit

A Anaya-Morales and F Delgado

Tecnologico de Monterrey, School of Engineering and Sciences, México.

E-mail: fdelgado@tec.mx

Abstract. Solving the electronic structure for multi-electronic systems is a hard problem. Even for small atoms and molecules, approximations have to be made in order to solve numerically the Schrödinger equation. Although different methods have been developed to take into account electron correlations, their computational cost reduces their feasibility. Quantum simulation provides an alternative to traditional computational methods for enquiring the electronic structure of molecules. Specifically, the Variational Quantum Eigensolver (VQE) algorithm provides a hybrid quantum-classical algorithm for the implementation on current near term quantum devices. In this work, we explore the implementation of VQE on Qiskit for calculating the ground-state energy of diatomic Hydrogen molecule.

1. Introduction

In 1929, Dirac remarked the mathematical difficulty of solving the equations arising from the quantum mechanical treatment of chemistry and physics [1]. Even for Helium, the second atom in the periodic table, we have to appeal to approximations [2, 3]. The complexity of whole chemistry arises from the two body terms describing the electron-electron interactions, which give rise to electronic correlations. In order to solve this, different methods were developed, giving rise to the area of computational chemistry [4–7]. With the emergence of quantum computers, chemistry proofs itself as a benchmark for simulating quantum systems on quantum devices [8–12], while offering an area for demonstrating quantum supremacy [13–15]. Although current devices are conditioned by the number of computational qubits available, error rates caused by quantum decoherence, and other physical limitations [16], still, the development of quantum error correction [17–19] and near term-quantum devices allow experimentally solve quantum chemical problems [20–22].

In this paper, we aim to introduce to the non-specialist public the applications of quantum algorithms, specifically the Variational Quantum Eigensolver (VQE) [10] in quantum chemistry for solving the H_2 molecule. Together, we show the implementation of such techniques on Qiskit [23].

2. Theoretical Background

When treating chemistry from a quantum mechanical approach, the first approximation to deal with is the Born-Oppenheimer (BO) approximation [24]. Under this, it is possible to decouple the nuclear and electronic wave-functions, treating the nuclei motion static relative to the electrons.

Therefore, the electronic Hamiltonian describing the dynamic of N electrons on the field of M point charges Z of static nuclei is [25–27]:

$$H_{elec} = -\frac{\hbar^2}{2m_e}\sum_{i=1}^{N}\frac{1}{2}\nabla_i^2 - k\sum_{i=1}^{N}\sum_{I=1}^{M}\frac{Z_I}{r_{iI}} + \frac{k}{2}\sum_{i=1}^{N}\sum_{j\neq i}^{N}\frac{1}{r_{ij}} + \frac{k}{2}\sum_{I=1}^{N}\sum_{J\neq I}^{M}\frac{Z_I Z_J}{R_{IJ}} \tag{1}$$

Where Z_I is the atomic number of each nucleus, r_{iI} stands for the separation distance between the i-th electron and the I-th nucleus, r_{ij} for the i-th and j-th electron relative distance, and R_{IJ} for the I-th and J-th nuclei separation. Also, k is the Coulomb constant while m_e is the electron mass. For most chemistry, the relevant unit of Energy is the Hartree $E_h = \frac{\hbar^2}{m_e a_0^2} = m_e c^2 \alpha^2$, with a_0 being the Bohr radius while c is the speed of light and α is the Fine-Structure constant. One Hartee is equivalent to 27.211 eV. In the following sections, we will drop the constants k and $\frac{\hbar^2}{2m_e}$ by working in the so called atomic units and discuss results in terms of Hartrees. The first term in equation (1) represents the canonical kinetic energy of the electrons. The second one, the coulombic attraction between the electrons and the nuclei. The third, corresponds to the repulsive electron-electron interaction. The last term accounts for the coulombic repulsion of nuclei, located at a fixed inter-atomic distance.

The whole electronic structure problem therefore reduces to an eigenvalue equation:

$$H_{elec}\Psi_{elec} = E_{elec}\Psi_{elec} \tag{2}$$

In 1927, Douglas Hartree introduced an iterative procedure known as the Self-Consistent Field (SCF) method for solving the Schrödinger Equation [4]. This procedure was improved by Slater and Fock [5–7] by applying the variational method, giving rise to the Hartree Fock (HF) theory. Together, they provide one of the standard methods used in quantum chemistry, the HF-SCF method. The heart of the HF theory relies on treating the electron-electron interactions as an average potential, reducing the many-body Schrödinger equation to the one-body Hartree-Fock equations [25,26]. The wave-function obtained from the HF method can be expressed as a Slater Determinant [25, 27], which carries the anti-symmetry condition of the wave-function [28, 29]. Although the wave-function from HF method is a good approximation, it does not represent the exact wave-function [27]. This is because the mean-field treatment of electron-electron interactions neglects the electronic correlations [30,31]. More sophisticated methods that include electronic correlations, known as post-HF methods, have been developed. These are the state of the art of current computational chemistry [26], however their computational cost makes them unfeasible for a broad range of applications.

As an alternative to post-HF methods, quantum algorithms have been recently proposed in order to enquire the electronic structure of atoms and molecules [10]. The basis of computation of quantum computing are abstract two level systems called qubits [32]. The quantum states of these qubits can be changed by applying unitary transformations, or quantum gates on them. In this way, Quantum computers exploit quantum phenomena like superposition and entanglement to speed up computation [33, 34].

The Variational Quantum Eigensolver (VQE) algorithm [10, 35] allows near-term quantum hardware to calculate the ground state energy of molecular systems. VQE is a hybrid algorithm which relies on both quantum and classical computers. Experimental realizations have been performed on photonic processors [10], superconducting devices [11, 36] and ion traps [37, 38]. The foundation of VQE lies on the Rayleigh-Ritz variational principle [39]. This principle states that any given trial wave function $|\Psi\rangle$ provides an upper bound to the ground state energy E_{gs} of a Hamiltonian H, that is:

$$E_{gs} \leq E_\Psi = \langle\Psi| H |\Psi\rangle \tag{3}$$

In VQE algorithm, it is attempted to construct a parameterized wave-function $\Psi(\vec{\theta})$ that approaches the exact ground-state wave-function Ψ_{gs}. For this, VQE relies on two subroutines, as shown in Figure 1. In the first subroutine, a quantum computer is used to prepare the parameterized state $\Psi(\vec{\theta})$ and measure it's energy expectation value $E(\vec{\theta})$. While on the second subroutine, a classical computer processes the results, optimizing and updating a new set of parameters $\vec{\theta}$ to be employed by the quantum hardware, providing an iterative process to calculate the ground-state energies of atoms and molecules.

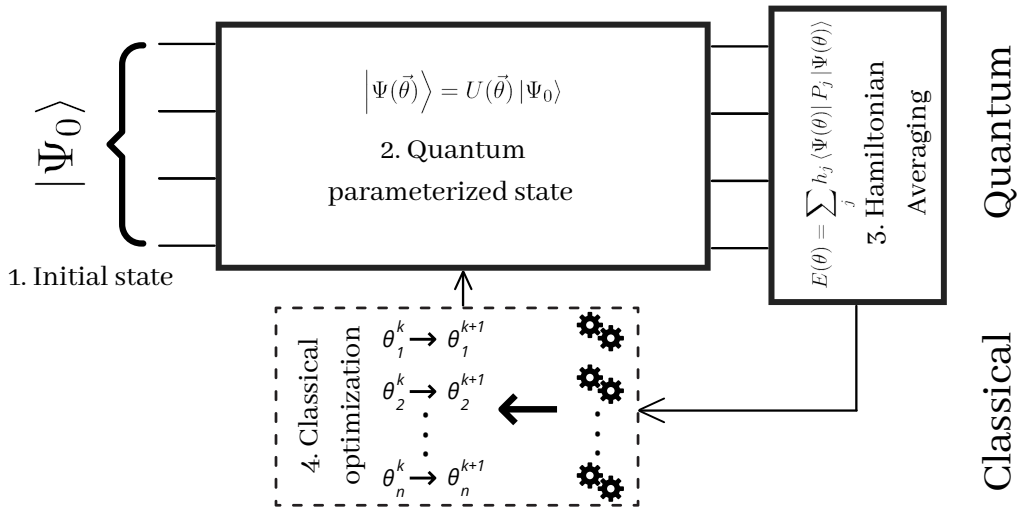

Figure 1: The Variational Quantum Eigensolver Algorithm consist of two subroutines. First, a parameterized quantum circuit consisting of single and two-qubit gates preforms an unitary transformation to an initial reference state. The expectation values of the Hamiltonian are measured following the Hamiltonian averaging procedure. The set of parameters and the calculated energy is given to a classical optimizer in order to generate a new set of optimized parameters to be given as input to the quantum circuit for further iterations until convergence is reached.

For the quantum state preparation, VQE employs a parameterized quantum circuit, denominated as Variational Form (VF). The action of this quantum circuit can be regarded as an unitary operation $U(\vec{\theta})$ that performs an unitary evolution on an initial reference state Ψ_0, generating a parameterized *anzats* wave-function $\Psi(\vec{\theta})$ as follows:

$$\left|\Psi(\vec{\theta})\right\rangle = U(\vec{\theta})\,|\Psi_0\rangle \tag{4}$$

Some of the initial states $|\Psi_0\rangle$ employed are the vacuum state $|0\rangle$ (which corresponds to initializing all qubits in the quantum circuit to the zero state), and the Hartree-Fock state (which is obtained by state preparation methods). Having an initial reference state that has significant overlap with the ground-state wave-function is desirable. In consequence, the Hartree-Fock as initial state is often used for chemical problems. Recently, methods for preparing multiconfigurational [40] and arbitrary Slater determinants [41, 42] as initial states have been explored.

The VF is characterized by a series of gates performing qubit rotations (R_x, R_y, R_z) and 2-qubit operations C_{NOT}, although other 2-qubit controlled gates can be used (in fact, a series

of universal gates reproducing any kind of computable process) [43]. The whole set of gate operations is called the layer. Then, the depth specifies the number of layers to be repeated on the quantum circuit. Increasing the depth increases the number of parameters to vary and therefore the range of the circuit to optimize the variational state. On the other hand, the entanglement setting specifies the configuration of the C_{NOT} gates. This can be linear, where C_{NOT} gates are applied to adjacent qubits; or full, with C_{NOT} gates applied to each possible qubit pair. An increase in the number of C_{NOT} gates increases the complexity of the circuit and the associated generation of entanglement in the global state, therefore, full entanglement is desired in principle. However, an increase on the number of quantum gates can led to the accumulation of gate errors and the increase of the evaluation time, making the qubits prone to decoherence [16]. Therefore a balance between these factors must be considered when choosing the depth and entanglement setting of the circuit for experimental implementations on quantum technologies.

Among the large variety of VFs, they can be classified in two: Hardware-efficient and chemical inspired [44]. Hardware-efficient VFs aim to reduce the number of parameterized gates, implementing gates that are available for the hardware. Although Hardware-efficient variational forms are the best alternative for current quantum devices, they are unsuitable for larger systems with significant electron correlations [12]. Moreover, initializing these VFs with random parameters can impede classical optimization [45]. Among the chemical inspired VFs, the Unitary Coupled Cluster (UCC) [46–48] can be implemented efficiently on quantum computers [37, 38, 49, 50]. UCC creates a parameterized trial state by applying excitations on an initial reference state. UCC is often truncated to single and double excitations becoming Unitary Couple Cluster Singles Doubles (UCCSD). Both Hardware-efficient and Chemically Inspired VFs are available on Qiskit. For further information consult their documentation [23].

Once the parameterized wave-function has been prepared, it is necessary to measure the expectation value of the Hamiltonian: $E(\vec{\theta}) = \left\langle \Psi(\vec{\theta}) \right| H \left| \Psi(\vec{\theta}) \right\rangle$. For this, the molecular Hamiltonian has to be expressed in the second quantization formalism using atomic units [25,27]:

$$
\begin{aligned}
H &= \sum_{pq} h_{pq} a_p^\dagger a_q + \frac{1}{2} \sum_{pqrs} h_{pqrs} a_p^\dagger a_q^\dagger a_r a_s \qquad (5)\\
&\text{with :} \quad h_{pq} = \int d\boldsymbol{x} \phi_p^\dagger(\boldsymbol{x}) (\frac{1}{2}\nabla_i^2 - \sum_{I=1} \frac{Z_I}{r_{iI}}) \phi_q(\boldsymbol{x})\\
&\qquad\quad h_{pqrs} = \int d\boldsymbol{x}_i d\boldsymbol{x}_j \frac{\phi_p^\dagger(\boldsymbol{x}_i)\phi_q^\dagger(\boldsymbol{x}_j)\phi_r(\boldsymbol{x}_j)\phi_s(\boldsymbol{x}_i)}{r_{ij}}
\end{aligned}
$$

where ϕ_p stands for the basis for the atomic orbitals, which can be found in [51]. In this formalism, the anti-symmetry of the wave-function is transferred from the Slater determinant onto the algebraic properties of the fermionic creation and annihilation operators, $a_p^\dagger$ and a_p respectively. This allow us to express the matrix elements of the Hamiltonian in terms of one and two body integrals, h_{pq} and h_{pqrs}. These integrals can be computed efficiently on quantum chemistry computational packages.

To this second-quantization Hamiltonian, it is performed a mapping from fermionic operators acting on indistinguishable electrons onto operators acting on distinguishable qubits. For example, mappings that allow to express the Hamiltonian in terms of products P of Pauli operators can be implemented on quantum devices and have become the standard procedure for quantum simulation. Among some of the mappings that have been developed, we found the Jordan-Wigner (JW) [52], Parity [53] and Bravyi-Kitaev (BK) [54] mapping schemes. By using these mappings, the one and two body integrals from equation (5) can be grouped in terms of h_j, which contains the information about the interactions of the Hamiltonian. Then, obtaining

the expectation values of the Pauli products P allow us to calculate the average energy $E(\vec{\theta})$:

$$H = \sum_j h_j P_j = \sum_j h_j \prod_{s_i \in S_j} \sigma_{s_i} \tag{6}$$

$$E(\vec{\theta}) = \sum_j h_j \left\langle \Psi(\vec{\theta}) \right| P_j \left| \Psi(\vec{\theta}) \right\rangle \tag{7}$$

there, each P_j is a product of Pauli matrices $\sigma_i, i = 0, 1, 2, 3$ in agreement with a sequence of numbers $S_j = \{s_1, s_2, ..., s_n\}, s_i = 0, 1, 2, 3$ for each qubit i considered in a circuit involving n qubits. The state preparation and measurement procedure is repeated to give an ensemble of N measurements. This procedure is known as Hamiltonian averaging [35] and reduces the decoherence error compared to other quantum simulation algorithms [55], however, in order to calculate the expectation value up to some precision ϵ, it is needed to perform $O(1/\epsilon^2)$ measurements [10]. In our development for the next section, we are considering $\epsilon \approx 0.18 - 0.25$ mainly guided by the processing-time performance.

Once the $E(\vec{\theta})$ is calculated, it is given as an input to a classical optimizer, together with the variational parameters $\vec{\theta}$. This classical optimization provides a new set of initial parameters for estimating the ground-state wave-function. The iterative optimization over the parameters allows to yield a closer value of the real ground state. Different numerical methods exist that have been employed in VQE applications. Qiskit Aqua components include both local and global local optimizers. Some of the later are: Constrained Optimization By Linear Approximation optimizer (COBYLA), which is useful whenever the derivative of the objective function is no known; Limited-memory BFGS Bound optimizer (LBFGSB), a quasi-Newton method; Sequential Least Squares Programming optimizer (SLSQP), which minimizes multi-variable function with a combination of constraints; and the Simultaneous Perturbation Stochastic Approximation (SPSA) optimizer, an stochastic gradient approximation recommended whenever measurement uncertainties are involved, like in quantum computation.

3. Case Study: H_2 molecule

Here, we will show first the implementation of a Single Point (SP) calculation of the H_2 molecule ground-state energy using the VQE algorithm on Qiskit. Then, we proceed to explore the Potential Energy Surface (PES) of the molecule by varying the variables of the VQE algorithm. Details of the code are provided in [56].

The H_2 molecule consist of two hydrogen atoms covalently bonded. The experimental bond distance corresponds to 0.740 Å [57]. This distance will be used to fix the positions of the atoms during the SP calculation, although arbitrary distances can be chosen. Qiskit employs PySCF quantum chemistry library for constructing a molecule driver (a programming subroutine in Python, please avoid a confusion with the "molecule" term non-related with our problem). This allows to obtain chemical information about the molecule. For constructing the driver, we must provide a computational basis set, the charge and spin multiplicity of the molecule. The driver allow us to extract the nuclear repulsion energy corresponding to the last term of equation (1), and calculate the one body and two body integrals in equation (5). For the VQE implementation, we also need to get from the driver the number of particles and spin orbitals.

After retrieving this information, we can map the molecular Hamiltonian to qubit operators by using the mapping methods available on Qiskit [52–54]. From here, we can construct an *ansatz*: an initial reference state (i.e. the zero state or the HF state) together with a VF. Combined, they are called an *ansatz* because both are required to produce the parameterized guess wave-function $\Psi(\vec{\theta})$. For its implementation in Qiskit, the *ansatz* requires as inputs: the mapping to be done, the number of particles and spin orbitals. These steps allow us to set up the

VQE circuit by using the VQE function, having as inputs the qubit operators, the *ansatz* and the classical optimizer. An initial set of parameters $\vec{\theta}$ can be randomly set, while intermediate calculations can be callback.

For the implementation, we used the STO-3G basis set, which stands for Slater Type Orbital formed by linear combination of 3 Gaussian functions. Basis sets in computational chemistry are used to approximate the atomic orbitals of elements in the periodic table. For further information, consult [51]. The molecule has zero charge and its ground-state corresponds to a singlet state of multiplicity of 1, setting these variables accordingly. We employed the Parity mapping, allowing us to reduce the problem from 4 to 2 qubits involving a representation of 5 Pauli products. The initial state chosen was the HF state and the variational form used was the UCCSD. We set the depth of the VF to 1 (caring the computational time needed for the evaluation). The VQE algorithm was carried out on a state vector simulator, which does not incorporate quantum noise, calculating the quantum state directly. The classical optimization was performed on the SLSQP optimizer. We callback the intermediate results in order to visualize the energy and parameter convergence, shown in Figure 2. Exact results where calculated using *Numpy* Eigensolver, which calculates the eigenvalues of the Hamiltonian and the smallest eigenvalue was taken as the Exact Energy corresponding to the ground-state. *Numpy* Eigensolver scales poorly with the size of the matrix and can only be used as reference for small systems.

Convergence was reached with an absolute error in the order of of 10^{-6} with respect to the *Numpy* eigenvalue calculation, giving a ground-state energy at the equilibrium of -1.13728 Hartrees, as shown inf figure 2a. Using computational Chemistry package available, for instance ORCA [58], we calculated HF result using the same basis set, obtaining a ground-state energy of -1.11751 Hartrees. We can see that VQE provides an improvement to the energy with respect to the HF method. Moreover, the calculation obtained with VQE is similar to those obtained by more sophisticated post-HF computational chemistry methods [59], like the ones obtained by Møller–Plesset Perturbation MP2/STO-3G (-1.13014 Hartrees), or the multi-configuratonal methods, like the Configuration Interaction CISD/STO-3G (-1.13731 Hartrees). Meanwhile, the experimental value for the H_2 dissociation is of 0.1749 Hartrees [60]. In general these methods are computationally expensive, even for molecules of few tens of atoms and therefore, and require bigger basis sets to converge to experimental values. However, the VQE algorithm doesn't depend that much on the basis, as the one and two body integrals are performed once during the whole algorithm. Therefore, VQE can allow us to construct quantum states that solve the correlation deficiency of HF theory without the computational cost of post-HF methods. The convergence of the parameters found in one of the evaluations, shown in Figure 2b, is consistent during different evaluations, converging around 30 iterations of the optimization process or less, showing the quantum speed up compared to classical computation.

While SP calculations at the equilibrium distance can give some insight about the convergence of VQE, it is of interest to study the PES by varying the inter-atomic distance between the hydrogen atoms. It is known that for larger distances far from the equilibrium position, H_2 molecule is poorly described by HF methods, and multi-configurational methods are required to give a better description of the molecule. This can be generalized for almost all chemistry. Therefore, we proceed to study the PES of H_2 using VQE. In Figure 3a, we show the PES for H_2 by using different mappings, specifically the parity mapping, the Jordan Wigner mapping and the Brayvi-Kitaev mapping. Although the three mappings perform accurately, it is possible to implement a qubit reduction procedure in the parity and the Brayvi-Kitaev mapping [36], providing the best options for applications in real quantum hardware. For the particular case of H_2, the qubit reduction does not affect the energy calculated, as it explodes the symmetry of the Hamiltonian, however, each molecule has to be considered as particular cases.

Another important aspect to take into consideration is the VF. In Figure 3b, we plot the

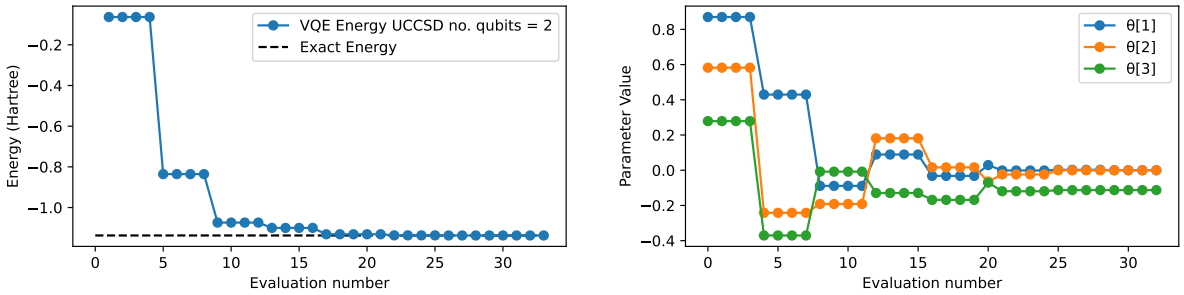

(a) (b)

Figure 2: (a) Energy convergence of the VQE implemented using the UCCSD variational form. (b) Parameter optimization convergence of the VQE circuit using UCCSD variational form.

PES of different VFs available in Qiskit. Specifically these were calculated using the chemically inspired UCCSD and the heuristic/Hardware-efficient Excitation Preserving, Real Amplitudes, Efficient $SU(2)$ and Two Local. We performed 30 calculations at each inter-atomic distance. The Excitation Preserving circuit preserves the ratio of $|00\rangle$, $|01\rangle$, $|10\rangle$ and $|11\rangle$ states. Meanwhile, the Two Local is a parameterized circuit consisting of alternating rotation layers applied to all qubits and entanglement layers. The Real Amplitudes has the characteristic that the prepared quantum states will only have real amplitudes. Finally, the Efficient $SU(2)$ variational form consists of single qubit operations spanned by $SU(2)$ group and C_X entanglement gates. For more description of the VF, look at Qiskit [23]. The initial parameters where randomly chosen at each point. For convenience we employ the Parity mapping, with a Hartree-Fock as initial state and the SLSQP optimizer. While the chemical inspired UCCSD VF performed correctly under different distances for random initial parameters, the Hardware-efficient VFs fluctuate at larger distances, being the Excitation Preserving the one with greater standard deviations at larger distances. Although this could be corrected by assigning as initial parameters the last values obtained on the algorithm, that increases the number of evaluations and therefore the evaluation times. Real Amplitudes and Efficient $SU(2)$ VFs show good behaviour at distances below the equilibrium, however, they start to show smaller deviations than the Excitation Preserving VF beyond that distance.

Furthermore, we inspect the behaviour of the optimizers given a Hardware-efficient variational form. For this, we employ the Efficient $SU(2)$, which shows small variations on the previous results. We tested the local optimizers COBYLA, LBFGSB, SLSQP and SPSA, since we expect that our ansatz is close to the ground-state. We evaluate at each distance 15 times to see the variation of the calculations at every point. Again, we mapped the molecular Hamiltonian using the Parity mapping and use the state vector simulator. These results are shown in Figure 3c. SPSA shows not only low precision, with standard deviations in the order of magnitude of the energies calculated, but also low accuracy, deviating from the exact energies calculated. LBFGSB and SLSQP optimizers shown little variations at inter-atomic distances above the equilibrium distance. COBYLA accurately calculated the results over the range of distances studied.

Finally, we explored the effect of quantum noise on the classical optimization by using the QASM simulator. This simulates a real quantum device execution, requiring a number of "shots" to provide the measurement statistics. The shots correspond to the number times that the quantum circuit is run to evaluate the probability distribution. Qiskit uses 1024 shots as default. It is important to note that previously, no shots were included, since the state-vector simulator assumed a perfect quantum device. Among the noise models, it is possible to costume

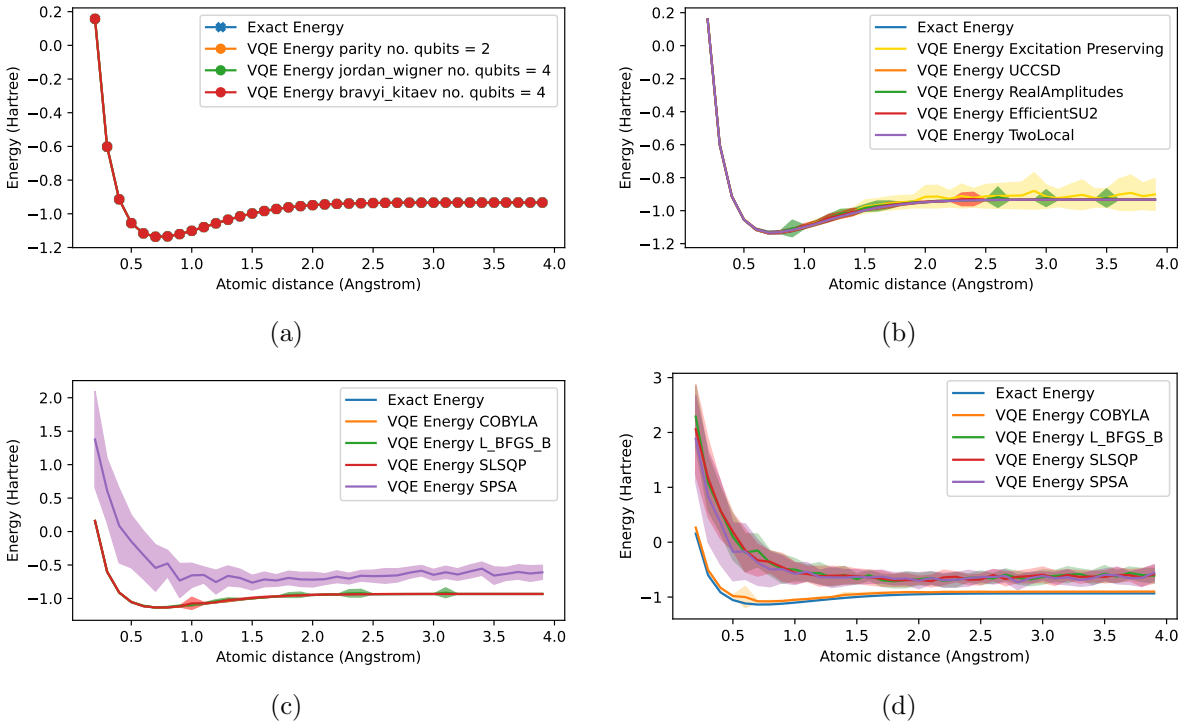

Figure 3: (a) Potential energy surface comparison of the VQE energies calculated for different mappings.(b) Potential energy surface comparison of the average energies calculated for different variational forms, the number of calculations performed at each point was set to 30. (c) Potential energy surface comparison of the average energies calculated for different optimizers, the number of calculations performed at each point was set to 15. The variational form implemented was Efficient $SU(2)$. (d) Similar experimental conditions from (c) were studied on QASM simulator incorporating noise model. In all plots, the filling region represents the standard deviation.

the circuit to include quantum errors to the circuit gates, readout errors to the measurements, thermal relaxations and depolarization of the quantum channels, among others. For the purpose of this work, we incorporate a noise model from the available quantum device at IBM Quantum experience: IBMQ Lima. This requires to provide the connectivity constraints of the qubits of the IBMQ device. By this, it is taken into account the 1 and 2 qubit gates errors, readout errors for each individual qubit, the decoherence times T_1 and T_2 and other properties obtained from the hardware. We performed 15 SP calculations at each bond distance in the EPS, with 8192 shots for each calculation. We again employ the same conditions as those from the previous experiment from figure 3c. The PES obtained is shown in Figure 3d. Only COBYLA optimizer shows accurate energies for the range of distances under consideration, however an increase on the standard deviation was observed for distances below the equilibrium. The rest of the local optimization methods have deviations in the order of magnitude of the energies. SPSA energies does not changed significantly from the noiseless calculations, proving its worthy under such conditions when error mitigation is included.

4. Conclusions

In this work, we provide an introduction to the application of VQE to electronic structure problems found in chemistry. We show the implementation on Qiskit and provide a comparison between different variables to consider while simulating the quantum algorithm. We observe

that both, the VF and the classical optimizer play a significant role on the calculations. It is known that VFs can only perform transformations over a subspace of the full Hilbert space. Therefore, the VF must be chosen such that the aimed state is found on the subspace spanned by the unitary transformation. Moreover, subspace reduction can be efficiently implemented in order to reduce the number of variational parameters and iterations for energy convergence [61]. The high dependency of hardware-efficient VFs to the initial parameters offset their advantage over chemically inspired ones, which are less prone to this random initialization. It is clear the necessity of developing chemically inspired variational forms that can be efficiently implemented on real devices in order to solve convergence problems. Meanwhile, the UCC provides a good chemical inspired variational form to test further more complex molecules [62].

On the same line, when running on real devices, optimizers must provide some protection against the random errors caused by decoherence and noisy environments. Altough SPSA optimizer has been highly recommended together with error mitigation schemes, in this study, COBYLA has shown excellent performance without the necessity of including error mitigation, therefore, further studies must be carried out on real quantum devices to test the performance of this optimizer.

While exact calculations using the eigenvalue methods like *Numpy* eigensolver can be used for small molecules, their use is unpractical for larger ones. More significant, VQE has shown improvements to the HF methods, and its results are comparable to the ones obtained by state of the art post-HF methods, showing the quantum advantage over standard quantum chemistry methods. Moreover, it is interesting to further explore the applications of VQE in systems where electron correlations are significant, like in transition metal complexes or excited states. The problem of electron correlations has been historically a barrier to overcome in the area of quantum chemistry by using classical computers, as they find hard to model quantum correlations, whereas highly entangled states are easy to produce on quantum devices. Therefore, further advances in the area must be carried out in this direction [40].

References

[1] Dirac P 1929 *R. Soc. London. Ser. A.* **123** 714
[2] Hylleraas E 1929 *Z. Phys.* **48** 469
[3] Hylleraas E 1929 *Z. Phys.* **54** 347
[4] Hartree D 1928 *Proc. Camb. Phil. Soc.* **24** 89
[5] Slater J 1928 *Phys. Rev.* **32** 339
[6] Slater J 1930 *Phys. Rev.* **35** 210
[7] Fock V 1930 *Z. Physik.* **61** 126
[8] Lloyd S 1996 *Science* **273** 1073
[9] Abrams D and Lloyd S *Phys. Rev. Lett.* **83** 5162
[10] Peruzzo A, McClean J and Shadbolt P et al 2014 *Nat. Commun.* **5** 4213
[11] Colless J, Ramasesh V, Dahlen D, Blok M, Kimchi-Schwartz M, McClean J, Carter J, de Jong W, Siddiqi and I 2018 *Phys. Rev. X* **8** 11021
[12] McCaskey A, Parks Z, Jakowski J et al 2019 *npj Quantum Inf.* 5 99
[13] Lund A, Bremner M, & Ralph T 2017 *Quantum Inf.* **3** 15
[14] Boixo S, Isakov S, Smelyanskiy V, Babbush R, Ding N, Jiang Z, Bremner M, Martinis J, and Neven H 2018 *Nat. Phy.* **6** 595
[15] Arute F, Arya K, Babbush R et al 2019 *Nat* **574** 505
[16] Ladd, T, Jelezko F, Laflamme R et al 2010 *Nat.* **464** 45
[17] Shor P 1995 *Phys. Rev. A* 52 2493
[18] Steane A 1996 *Phys. Rev. Lett.* 77 793
[19] Preskill J 1998 *R. Soc. Lond. A.* **454** 385
[20] Kandala A, Mezzacapo A, Temme K et al 2017 *Nat.* **549** 242
[21] Nikolaj M et al 2018 *Quantum Sci. Technol.* **3** 30503
[22] Kandala A, Temme K, Córcoles A et al 2019 *Nat.* 567 491
[23] Gadi Aleksandrowicz et al 2019 Qiskit: An Open-source Framework for Quantum Computing (0.7.2) Zenodo https://doi.org/10.5281/zenodo.2562111

[24] Born M and Oppenheimer J 1927 *Ann.Physik* **84** 457
[25] Szabo A and Ostlund N 1996 *Modern Quantum Chemistry: Introduction To Advanced Electronic Structure Theory* (Mineola N.Y: Dover Publications)
[26] Cramer Ch 2002 *Essentials of Computational Chemistry* (Chichester: John Wiley & Sons)
[27] Helgaker T, Jørgensen P, and Olsen J 2000 *Molecular Electronic-Structure Theory* (Chichester: John Wiley & Sons)
[28] Slater J 1929 *Phys. Rev.* **4** 1293
[29] Slater J 1931 *Phys. Rev.* **38** 1109
[30] Wigner E 1934 *Phys. Rev.* **46** 1002
[31] Löwdin P 1955 *Phys. Rev.* **97** 1509
[32] Nielsen A and Chuang I 2010 *Quantum Computation and Quantum Information* (New York: Cambridge University Press)
[33] Rieffel E and Polak W 2011 *Quantum Computing: A Gentle Introduction* (Massachusetts: The MIT Press)
[34] Kaye P, Laflamme R, and Mosca, M 2010 *An introduction to quantum computing* (Oxford: Oxford University Press)
[35] McClean J et al 2016 *New J. Phys* **18** 023023
[36] O'Malley P et al 2016 *Phys. Rev. X.* **6** 031007
[37] Hempel C, Maier C, Romero J, McClean J, Monz T, Shen H and Roos C 2018 *Phys Rev X***8**(3)
[38] Shen Y, Zhang X, Zhang S, Zhang J, Yung M, and Kim K 2017 *Phys. Rev. A* **95** 020501
[39] Griffiths D 2005 *Introduction to quantum mechanics* (New Jersey: Pearson Prentice Hall)
[40] Sugisaki K, Nakazawa S, Toyota K, Sato K, Shiomi D, and Takui T 2019 *ACS Cent. Sci.* **5** (1) 167
[41] Babbush R, McClean J, Wecker D, Aspuru-Guzik A, and Wiebe N 2015 *Phys. Rev. A* **91** 022311
[42] Jiang Z, Sung K, Kechedzhi K, Smelyanskiy V, and Boixo S 2018 *Phys. Rev.* **9** 044036
[43] Barenco A, Bennett Ch, Cleve R, DiVincenzo D, Margolus N, Shor P, Sleator T, Smolin J, Weinfurter H 1995 it Physical Review A **52** (5) 3457–3467
[44] McArdle S, Endo S, Aspuru-Guzik A, Benjamin S, Yuan X 2020 *Rev. Mod. Phys.* **92** 15003
[45] McClean J, Boixo S, Smelyanskiy V, Babbush R, and Neven H 2018 *Nat. Comm.* **9** 4812
[46] Bartlett R, Kucharski S, & Noga J 1989 *Chem. Phys. Lett.* **15** (1) 133
[47] Hoffmann M R and Simons J 1988 *J. Chem. Phys.* **88** 993
[48] Taube A G & Bartlett R J 2006 *Int. J. of Quant. Chem.* **106**(15) 3393
[49] Ryabinkin I G, Yen T C, Genin S N, and Izmaylov A F 2018 *J. of Chem, Theo. and Comp.* **14** (12) 6317
[50] Romero J et al 2018 *Quant. Sci. Technol.* **4** 014008
[51] Schuchardt, K L , Didier, B T, Elsethagen, T, Sun, L, Gurumoorthi, V, Chase, J, Li, J, and Windus, T L 2007 *J. Chem. Inf. Model* , **47**(3), 1045-1052
[52] Jordan P, Wigner, E 1928 *Z. Physik* **47** 631
[53] Bravyi S, Gambetta J, Mezzacapo A, and Temme K 2017 *arXiv:1701.08213*
[54] Bravyi S B & Kitaev A Y 2002 *Ann. of Phys.* **298**(1) 210
[55] Harrow A W, Hassidim A, and Lloyd S 2009 *Phys. Rev. Lett.* **103** 150502
[56] Anaya A, Delgado F 2022 *arXiv:quant-ph/2201.04216*
[57] Orville-Thomas W J 1980 *J. of Mol. Str.* **64** 299
[58] Neese F, Wennmohs F, Becker U, and Riplinger U. 2020 *J. Chem. Phys.* **152**, 224108
[59] NIST Computational Chemistry Comparison and Benchmark Database. NIST Standard Reference Database Number 101. http://cccbdb.nist.gov/ DOI:10.18434/T47C7Z
[60] Hirschfelder J O and Linnett J W 1950 *J. Chem. Phys.* **18**, 130-142
[61] Zhang F, Gomes N, Berthusen N, Orth P P, Wang C, Ho K, and Yao Y X 2021 *Phys. Rev. Research* **3** 013039
[62] Wecker D, Hastings M B, Troyer M 2015 *Phys. Rev. A* **92** 042303